TABLE OF CONTENTS

1. Tandem-X, an Emergency-Response Flyer

In the realm of emergency-response air vehicles, rapid dispatch and subsequent transit to the scene – by ground or directly by air – are highly desirable qualities. So too would be the vehicles' abilities to penetrate dense, obstacle-laden environments (e.g., trees, buildings, hydro wires), hover for extended periods in punishing weather, and take off and land in extreme terrain – all while carrying the injured and supplies. We introduce an aircraft capable of all these undertakings – characterized by the GoAERO Prize – and more: the Tandem-X Flyer depicted in Figure 1 and described in the following pages.

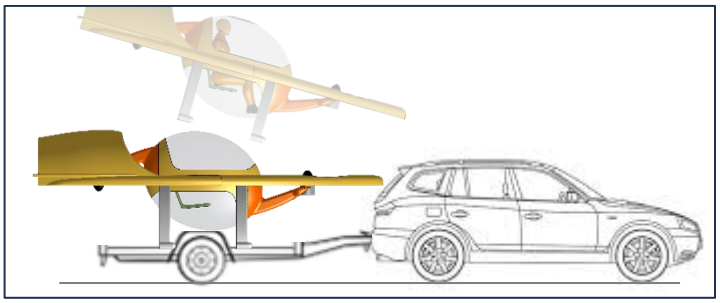

(a) Flyer is roadable (Sect. 2.3.5) and ready to take off without adjustment or preparation upon arrival at scene.

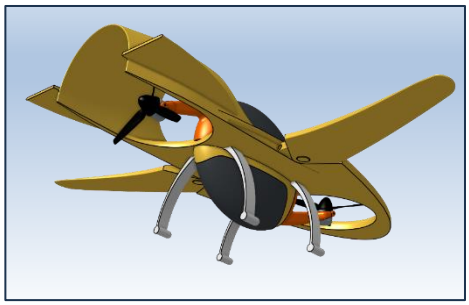

(b) But can travel far on its own as well, with substantial payloads (Sect. 5.3.1).

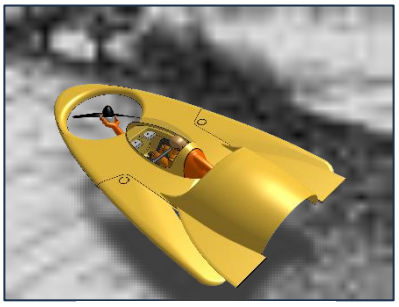

(c) Takes off and lands from severely inclined surfaces. Prop discs stay horizontal. (Sects. 3.3 and 3.6).

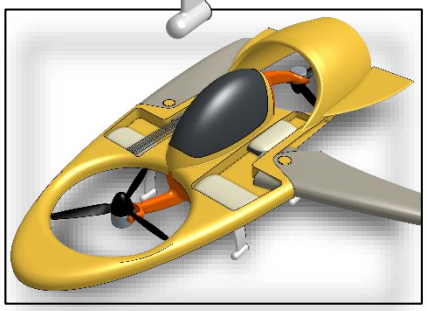

(d) Has 10 ft^3 cargo vol + occupant enclosure, Mission 1. (Sect. 3.2.3 offset payloads, 4 Structures, 5 Performance).

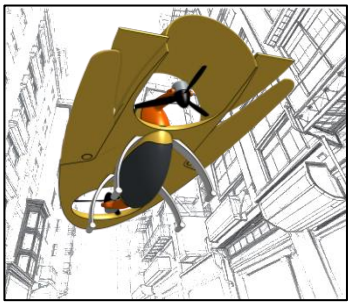

(e) Is narrow & smooth for dense environments (Sects. 2.3.1-2.3.2). Underside observation window.

Figure 1. *Center*: eVTOL Tandem-X Flyer dual-propeller concept drawing with inset detail. *Peripheral images:* (a) through (e) depict some of the Flyer's main features, with references to sections in remainder of report.

2. Aircraft Technical Overview

The Flyer is an eVTOL aircraft comprising two swivelling lift-propellers arranged in a narrow-environment tandem configuration and enveloped by an arrow-shaped lifting fuselage. The counter-rotating, fixed pitch propellers are directly driven by electric motors situated on gimballed mounts, which can be actively tilted in all directions by servos to effect aircraft control in hover, and propulsion for forward flight.

2.1 More-than-Effective Hover Control

Throttle changes and tilt rates, together with the propellers' drag torques and mass moment of inertias (MMoAs) respectively, create sharp, gust-penetrating propeller-torque and gyroscopic control moments – supplementing the conventional static ones from thrust and obviating the need for more than two lift propellers. More than this, the system provides six-axis independent control, enabling abilities like stationary pitching and its opposite: forward motion without pitching. Such control will be described in more detail in Section 3.

Generally, an onboard flight controller receives attitude-sensor and command signals from an autonomous navigation system or human pilot (remote or onboard), and sends appropriately-mixed ones to the tilt servos and the prop-motor speed controls to ensure stability of the aircraft at all times during controlled flights. Since a human pilot must be remote in the GoAERO Prize, this control will be enabled – and close proximity with the environment facilitated – through a first-person view (FPV) system with head-motion sensors embedded in the pilot's view-goggles, and corresponding tracking camera(s) situated onboard.

2.2 Wingborne Flight, Lifting-Body Mode and High-Speed Dash

The Flyer also comprises variable sweep wings which are normally swept back in hover mode, allowing low-altitude, close-environment maneuvering while off-loading the propellers slightly when travelling forward in that mode. With wing sweep being only ground-adjustable in the Go AERO Prize (for the sake of simplicity and weight in carrying out the separate missions), this is also how the Flyer begins it's extended-wing flight – by moving forward in the air from near-zero velocity. Tilting one or both propellers further increases forward speed, with the propeller thrusts being (automatically) adjusted to maintain the Flyer's horizontal attitude. Sustained forward flight in full airplane mode is manifested by the wings bearing the full aircraft weight and at least one of the propellers tilted fully forward 90 degrees. Control in airplane mode is conventional, with ailerons in the wings and elevators at the rear of the horizontal stabilizers attached to the half-duct (more on this item below). The propellers are not laterally tilted in airplane mode for control.

There is also a high-speed dash mode for the Flyer (which is accomplished more easily with an onboard wing-sweep actuator) where the wings are swept back from airplane mode with the power high and both propellers tilted forward 90 degrees. For this same high power, the swept-wing Flyer will be faster than it is in airplane mode, and this is outlined in Sect. 5.2.2. Though difficult to operate in in its mid-velocity range because of the very high angles of attack involved, this flight realm with swept-back wings is in fact continuous, from near-zero velocity – and providing lift assistance to the Flyer in hover mode – to encompassing high-speed dash with the aforementioned high speeds. Here referred to as *lifting-body mode*, it's performance is investigated and plotted in Sect. 5.2.

2.3 Configuration Reasoning

The following sections outline the main rationalizations behind the Flyer's design for the GoAERO Prize.

2.3.1 Tandem Birotor: Best Hover Endurance for Given Width

It is envisioned that an emergency-response flyer should be narrow in planform to better penetrate obstacle-laden or dense environments such as forests, urban areas, and mountainous terrain. Referring to Fig. 2, for a given vehicle width, then, lift propellers arranged in tandem will allow their maximum possible diameter, D_m, giving a birotor a total disc area of $0.5\pi D_m^2$. In comparison, a quadrotor's propeller diameter will be only about $0.5D_m$, and it's total disc area $0.25\pi D_m^2$ – half the birotorster's. For the same take-off weight, therefore, the quadrotor's hover endurance will be much less than the birotor's. And though its empty weight might in fact be half the birotor's – making its empty-weight disc loading the same – the quadrotor must carry the same equipment and payload as the birotor, and therefore its operational disc loading will always be higher and it's endurance always less.

The one obstacle normally excluding birotors from eVTOL applications is their apparent lack of hover stability, but, as will be shown in Sect. 3, this has been more than overcome with the use of the propellers as gyroscopes and momentum wheels – such that there are in fact control advantages to using birotors.

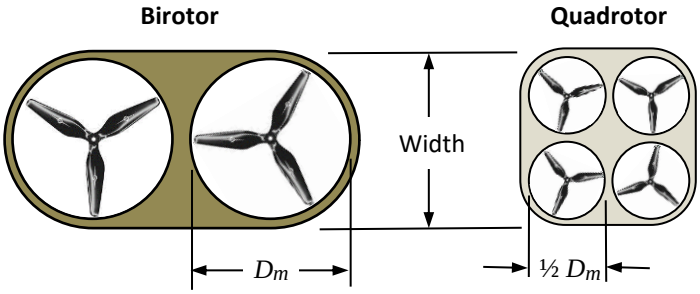

Fig. 2. Quadrotor propeller diameter and total disc area are half that of same-width birotor's.

2.3.2 Shrouded Propellers for Safety

To avoid blade strikes with objects in the environment and also ensure the safety of ground personnel, the propellers in the proposed aircraft needed to be shrouded, or embedded in its fuselage, wing, or wing-body. Propeller shrouds improve hover performance – through the fan-in-wing effect, discussed in Sect. 5.1.1 – and are here considered critical for operating in the confined emergency-response environments that the GoAERO Prize represents.

2.3.3 Horizontal Lifting Surfaces for More Efficient Forward Flight

Since VTOL emergency-response aircraft need to travel to a destination in order to perform their task(s), they can benefit from horizontal lifting surfaces which utilize this forward motion and off-load the (lift) propellers. As shown in Fig. 3, these surfaces are incorporated as a portion of the given overall aircraft width dictated by the aircraft's storage and transport considerations and discussed in the sections to follow.

Concerns for confined-environment penetration, the aerodynamic center's location, and delayed stalling of the lifting surfaces has determined the semi-elliptical planform shape of the aircraft's body shown in Fig. 3. There is no lifting surface or shroud shown aft of the rear propeller in the body; it has been omitted in anticipation of tilting the rear propeller forward 90 degrees for a more-efficient airplane mode – without adverse airstream impingement during the transition. Any lost lifting surface-area is compensated by incorporation of the half-duct discussed in the next section.

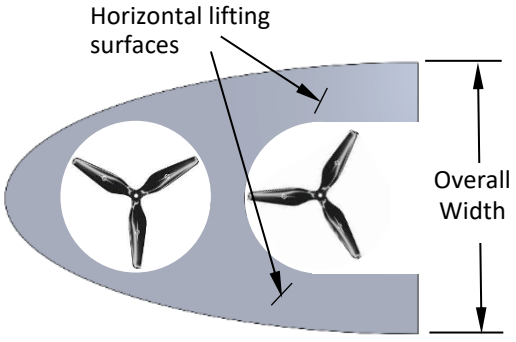

Fig. 3. Body shape for confined-environment penetration and off-loading of lift propellers.

2.3.4 Half-Duct for Lift, Stabilization and Added Safety

The half-duct situated over and around the rear propeller, as shown on the left side of Fig. 4, adds a measure of safety in near-ground operations and in the use of a ballistic parachute for in-flight recovery. It also provides lift in forward flight and acts as a vertical and horizontal stabilizer. The

half-duct closely encases the rear propeller when tilted forward the full 90 degrees from its hover position, and can augment lift further in this condition due to the *inverse Custer effect* (Ref: Gress, "Transitioning eVTOL aircraft with augmentative cross-modal elements", VHS Forum 80, 2024).

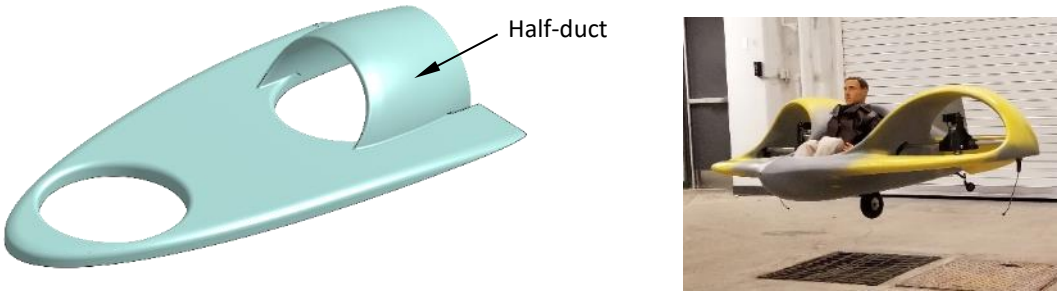

Fig. 4 *Left*: Proposed GoAERO aircraft with half-duct at rear. *Right*: Hovering GoFly side-by-side birotor 1/3-scale prototype with half-ducts (Gress/Athena Aero, 2019).

As shown on the right side of Fig. 4, the feasibility of the half-duct in hover has been demonstrated by the team author's 1/3-scale, side-by-side birotor prototype made for the GoFly competition (Gress/Athena Aero, 2019). Though accurate measurements were not made, there appeared to be little or no degradation in indoor hover performance due to the presence of the half-ducts.

2.3.5 Flight-Ready Roadability, and Flyer Storage, Flight Efficiency, Length

To minimize emergency response time, the Flyer is intended to be flight-ready while atop an open trailer in transit to the (take-off) site; i.e., without having to assemble or add flight-enabling components. With this constraint, referred to as the *roadable* condition, the Flyer's overall width cannot be more than 8.5 ft. (102 in.) (Fig. 5). To ensure that some horizontal surface area is still

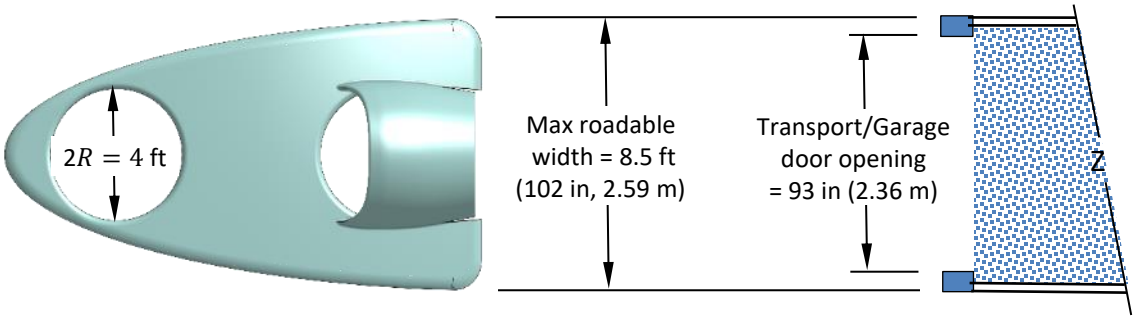

Fig. 5. Maximum overall width of 8.5 ft. (102") for a roadable, ready-to-fly GoAERO Flyer. Compare to door opening of 93" for storage garage or enclosed tractor trailer.

available to provide more efficient lift in forward flight, and to allow for the wing introduced in the next section, the propellers' diameter is limited to 4 ft. (tip radius R = 2 ft. for the analytical work in upcoming sections). As will be seen, the fan-in-wing effect – and the actual wing – will offset the propellers' relatively small size in terms of flight efficiency.

The aircraft's overall width cannot be fixed at 8.5 ft (102 in.) however, for as also shown in Fig. 5, the door opening of a storage garage with a nominal 8 ft. door – and of an enclosed tractor trailer for long-distance transport – is only 93 inches wide. Rather than reduce the Flyer's 102 in. design-width and performance to accommodate this door constraint, it had been decided to commit to a variable-geometry wing, one that not only swings outward for flying as an airplane, but also inward from the hover/roadable condition to pass through such doors when necessary.

Finally, the Flyer's length of approximately 16 ft. is largely the outcome of enveloping the two 4-ft. propellers and providing about 6 ft. between them for the GoAERO payload requirements.

2.3.6 Variable-Sweep-Wing Modes: Storage; Road/Hover; Airplane; and High-Speed Dash

Figure 5 shows the three basic modes of: storage; road/hover, and; airplane – along with their associated widths – and how they are facilitated using variable-sweep wings and selected pivot points.

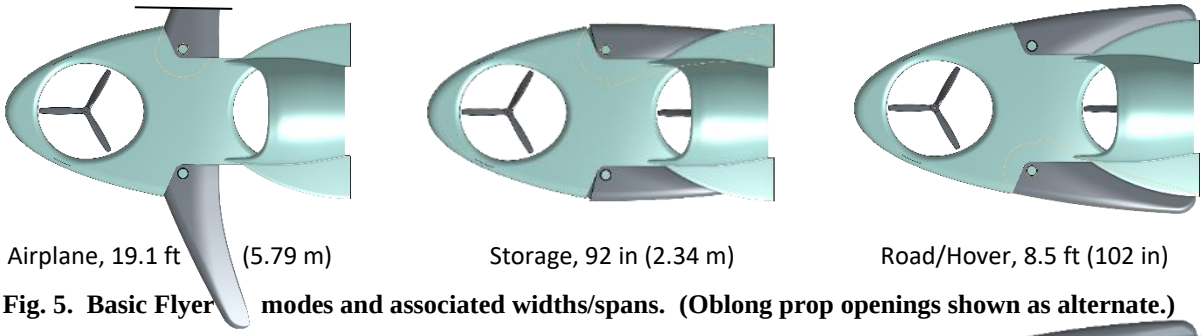

Fig. 5. Basic Flyer modes and associated widths/spans. (Oblong prop openings shown as alternate.)

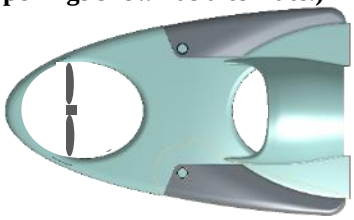

Fig. 6. High-speed dash mode, with both propellers tilted forward 90 degrees.

The high-speed dash mode, referred to earlier and wherein the propellers are tilted 90 degrees forward, is shown in Fig. 6. From both Figs. 5 and 6 it is evident that the wings are essentially fully exposed in all flying modes, and that their shape and size are dictated by their collapsed, hover-mode form. The wingspan in airplane mode is largely determined by the aircraft's length. Similarly, the wing taper is dictated by the available space between the aircraft's hover-mode outer edge and rear propeller's blade tips – and the horizontal stabilizers now affixed to the half-duct. Despite these constraints, the wings in airplane mode extend the aircraft's range and endurance substantially, possibly making ground transport unnecessary in many real-life cases (Sect. 5.3).

3. Stable Hovers with Aerodynamic and Inertial Propeller Moments

The following describes control of the birotor Flyer in hover mode, which is achieved solely by the manipulation of its counter-rotating propellers' spin rates and their spin-axis directions, i.e., tilting in all directions. A brief description of the mechanics of such tilting is deferred to Sect. 4.

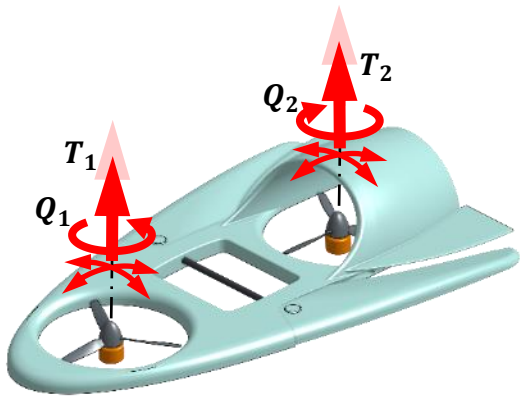

Fig. 7. Varying only aerodynamic vectors provides insufficient birotor control authority in hover. Inertial moments are required as well. (Note: A schematic Flyer is shown here and throughout this section.)

The aforementioned manipulation not only varies the propeller thrust and torque vectors ($\boldsymbol{T_{1,2}}$ and $\boldsymbol{Q_{1,2}}$, Fig. 7) – conventional aerodynamic elements whose response speeds and magnitudes are insufficient to provide full birotor control authority – it also generates inertial moments which provide the missing dynamic control elements. In this aircraft the propellers are utilized as momentum-wheels and control moment gyroscopes, critical inertial elements normally used for attitude control in the realm of space flight. The following discusses this utilization for each of the aircraft's three control axes.

3.1 Roll Control from Gyroscopics and Drag Torques: Opposed Longitudinal Tilting

Due to its mass moment of inertia (MMoI) about its spin axis, a propeller generates a gyroscopic moment while it is being tilted – a much greater one than that needed to tilt it. The moment's direction, using the right-hand rule, is perpendicular to the propeller's spin and tilt axes (or vectors), and its magnitude is the product of its MMoI (I_R), its spin speed (ω), and its tilt rate. Referring to Fig. 8, roll ϕ of the Flyer is dynamically controlled by the propellers' gyroscopic moments $I_R\omega_i\beta'$ arising from their simultaneous tilting at rates β' in opposite longitudinal directions.

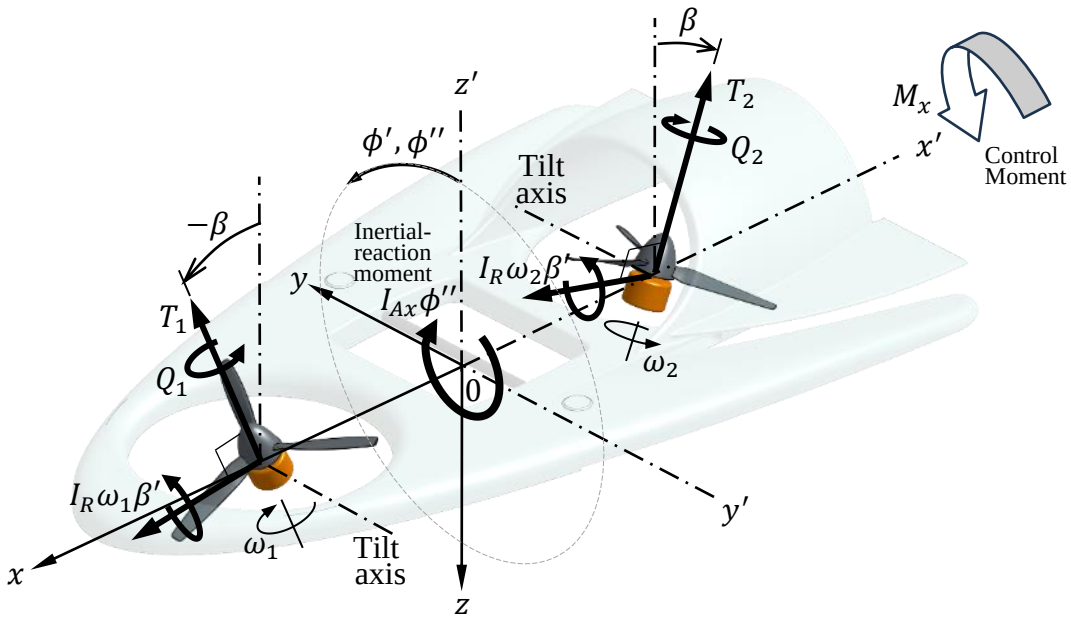

Fig 8. Effecting roll ϕ using gyroscopic moments $I_R\omega\beta'$ and drag torques Q from propellers' simultaneous tilting in opposite longitudinal directions.

The full roll-control moment, M_x, is completed with the inclusion of the static moments acting on the aircraft, i.e., the propeller drag-torque reactions Q_i. Projecting all of the propeller moments onto the aircraft roll axis xx', and assuming that the parameters ω_i and Q_i are identical for the two propellers – and now referred to as parameters ω and Q respectively – in this simple study, gives the full roll-control moment as

$$M_x = 2I_R\omega cos\beta \cdot \beta' + 2Qsin\beta \cong 2(I_R\omega\beta' + Q\beta) \quad \text{for small } \beta \ (< 15°) \quad (1)$$

3.2 Roll Stability

The equation of motion in roll derives from equating the control moment M_x to the aircraft's inertial-reaction moment $I_{Ax}\phi''$. Assuming a simple proportional sensor-and-tilt-servo controller of the form $\beta = -k_{\phi p}\,\phi$, where $k_{\phi p}$ is its gain, the equation of motion in terms of ϕ becomes

$$\frac{I_{Ax}}{2k_{\phi p}}\phi'' + I_R\omega\phi' + Q\phi = 0 \quad (2)$$

which is second-order, with positive, non-zero coefficients, and so represents a stable system.

3.2.1 Minimum Servo Speed

To enable roll stability practically, the tilt servos' speeds should be greater than the system's undamped natural frequency, which is determined from the square root of the ϕ and ϕ''-coefficient ratio in Eqn. (2):

$$f_n \;=\; \sqrt{\frac{2k_{\phi p}Q}{I_{Ax}}} \tag{3}$$

Values for f_n of the author's past, 1/3-scale prototypes (of a personal eVTOL flyer) are about 1 rad/sec, slower than their hobby servos' 60°/0.15 sec. For full-size, geometrically similar aircraft, f_n will be $\sqrt{S}$ times slower than models', where is S is the scale factor (= 3). Dividing, this gives a full-size natural frequency of about 0.58 rad/sec (33°/sec), which the larger servos must surpass.

3.2.2 Minimum Propeller Mass Moment of Inertia and Minimum Tilt-Servo Torque

Oscillations disappear when the system is critically- or over-damped (damping ratio in Eqn. (2) ≥ 1), whose desirability gives one an idea of the propellers' required spin inertias I_R:

$$I_R \;\geq\; \frac{1}{\omega}\sqrt{\frac{2I_{Ax}Q}{k_{\phi p}}} \tag{4}$$

Again using the author's past 1/3-scale prototypes, Eqn. (4) gives a minimum I_R of 0.0007 ft-lb-sec^2, compared to 0.0016 ft-lb-sec^2 for the propellers actually used (16x10" Master Airscrew 3-bladed). An estimate of the minimum required servo torque – to resist gyroscopic back-moments resulting from rolling of the aircraft – is the product $I_R\omega f_n$ which, from (3) and (4), is simply $2Q$, and equal to a reasonable 256 oz-in for the 1/3-scale prototypes, which use servos of 350 oz-in capacity (Hitec HS-7955TG). Mass-moment of inertia increases with the fifth power of scale factor (i.e., S^5), which gives a minimum I_R of 243 x 0.0007 = 0.17 ft-lb-sec^2 for the full size Flyer, indicating a reasonable minimum weight of 2.4 lb for the 4-ft. dia. propeller (based on a radius to the equivalent point-mass of 0.75R = 1.5 ft.). However, in Sect. 5.1.1, the propeller rotational speed will be reduced by a factor of 1.5, so from Eqn. (4) the minimum weight of the propeller is actually 3.6 lb. (1.6 kg), a still reasonable value (and which corresponds to the increase in blade chord which caused the speed reduction). For selecting the full-size servo actuator, the $I_R\omega f_n$ product (or $2Q$) scales with S^4, so its minimum torque is (81x256 =) 20,736 oz-in = 108 ft-lb (146 Nm).

3.2.3 Handling an Offset Payload

A payload of weight W_P and offset laterally by distance u can be balanced – and roll equilibrium maintained in the steady state – by the drag-torque roll components resulting from an equal and opposite longitudinal tilt β of the propellers (Fig. 9). Using the exact relation in Eqn. (1) and equating moments acting about the longitudinal axis gives

$$(M_x =) \quad 2Qsin\beta \;=\; uW_P \tag{5}$$

A simple static thrust-torque relation for a group of geometrically similar, fixed-pitch propellers – or of a single propeller whose rotational speed can be varied – is

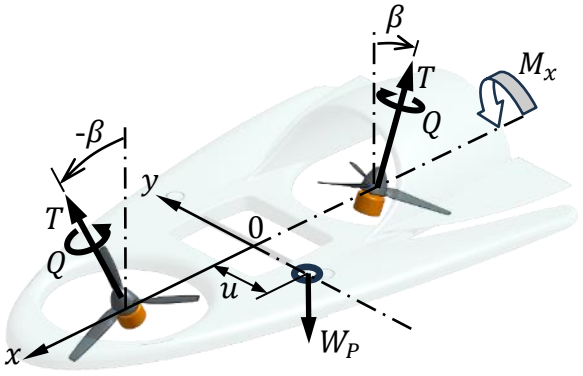

Fig. 9. Balancing laterally offset payload with drag-torque roll-components $Qsin\beta$.

$$Q \;=\; c_q R \cdot T \tag{6}$$

where R is the propeller tip radius, and the unitless coefficient c_q is specific to the type (= 0.2 for 3-bladed MA propellers). If T_0 is the hovering thrust of each propeller before the offset payload is applied, then its hovering thrust T with the added payload is

$$T \;=\; \left(T_0 \;+\; \tfrac{1}{2}W_P\right)/cos\beta \tag{7}$$

Eliminating T in (6) with (7), and with the result eliminating Q in (5), produces the relation for tilt angle β in terms of the payload parameters and initial conditions:

$$tan\beta \;=\; \frac{u{\cdot}W_P}{c_q R(2T_0 + W_P)} \;=\; \frac{250}{2T_0 + 125} \qquad (8)$$

where the numerical ratio on the right side represents the specific case of a flyer with 4 ft. diameter propellers in the MA 3-bladed propeller group ($c_q = 0.2$), and using the 'Alex' mannequin for payload ($W_P = 125$ lb.), with a lateral offset of half a human adult's shoulder width (for potential side-by-side seating) so that $u = 10$ in. $= 0.8$ ft. Table 1 lists β and T for a range of T_0 using Eqn. (8) and (7), which shows β to be just over 25 deg. for a 400 lb. aircraft, the angle reducing as the empty aircraft gets heavier. As well, comparing the last two columns, there is a necessary but slight thrust increase due to that angle.

Table 1. Fore-aft tilt β to balance payload W_P=125 lb, offset lateral distance u = 0.8 ft, using torques Q. Offset requires slight thrust increase.

$2T_0$ (lb)	β (deg)	$2T_0 + W_P$	$2T$ (lb)
400	25.5	525	582
500	21.8	625	674
600	19.0	725	766
700	16.9	825	862
800	15.1	925	958
900	13.7	1025	1056
1000	12.5	1125	1152

3.3 Collective Lateral Tilting for Special Roll Operations

Another element of control is thrust vectoring via the propellers' simultaneous lateral tilting in the same direction (angle γ in Fig. 10) – referred to simply as collective lateral tilting. Such thrust vectoring can simply effect lateral motion of the aircraft independently of roll or, with a low aircraft center of mass relative to the propeller tilt axes (distance h in Fig. 15), supplement the roll-control moment M_x of Sect. 3.1. From Fig. 15, this thrust-vectoring roll-control moment is

$$M_{Tx} \;=\; 2hTsin\gamma - 2I_P\gamma'' \qquad (9)$$

where I_P is the MMoI of the propeller pod resisting its tilting – a potentially destabilizing element which must be minimized or accounted for. In general, collective lateral tilting γ and opposed longitudinal tilting β can be combined (electronically) in several ways to provide

- increased roll, coupled with lateral motion.
- lateral motion without roll.
- stationary roll, i.e., propeller disks remain in horizontal plane

Finally, it is noted that the drag torques and gyroscopic moments from the two propellers cancel one another during collective lateral tilting.

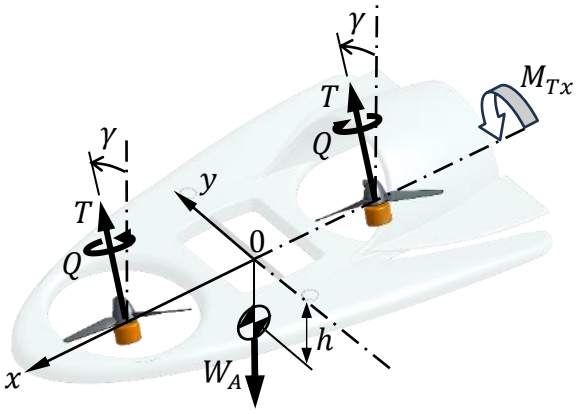

Fig. 10. Lateral thrust vectoring from collective lateral tilting for supplemental roll control, lateral motion without roll, and stationary rolls.

3.4 Augmenting Pitch and Yaw by Decoupling: Differential Thrusts and Lateral Tilts

Pitching by angle θ of the tandem birotor can derive from a thrust differential $T_1 - T_2$ between its propellers (arising from a speed differential $\omega_1 - \omega_2$), a common method of controlling multi-copters about their horizontal axes. Such a differential in a birotor, however, incurs a corresponding propeller torque imbalance of $Q_1 - Q_2$, causing yawing ψ of the aircraft as well. To prevent this, the propellers must be differentially tilted in the lateral direction simultaneously – as shown in Fig. 11. Fortuitously, this tilting augments the original intended pitching (with propeller torque and gyroscopic components), with the full pitch-control moment now being

$$M_y \;\left(= I_{Ay}\theta''\right) = \; l(T_1 - T_2)cos\gamma \;+\; I_R(\omega_1 + \omega_2)cos\gamma \cdot \gamma' \;+\; (Q_1 + Q_2)sin\gamma \qquad (10)$$

$$\cong \; l(T_1 - T_2) \;+\; I_R(\omega_1 + \omega_2)\gamma' \;+\; (Q_1 + Q_2)\gamma \qquad (\gamma < 15°) \quad (10')$$

where the augmentative elements are in blue.

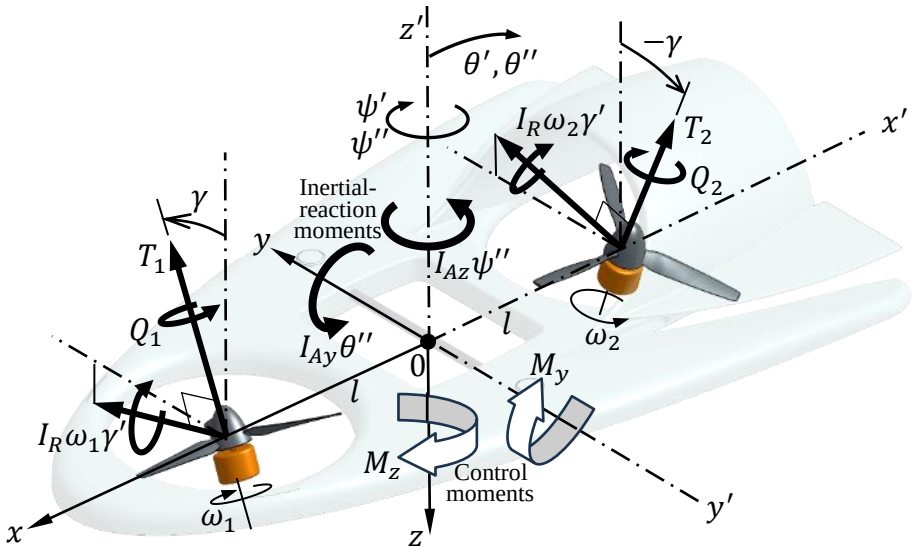

Fig. 11. Pitch and yaw control from differential thrusts, torques and lateral tilts.

Similarly, as already indicated, differential lateral tilting to effect yaw control will also incur unwanted pitching moments (from the propeller torques and gyroscopic moments). Preventing this requires a thrust differential and therefore propeller speed and torque changes, the latter then augmenting the intended yaw – as seen in the linearized relation for the full yaw-control moment:

$$M_z \ (= I_{Az}\theta'') \ = \ l(T_1 + T_2)sin\gamma \ + \ I_R(\omega_1 - \omega_2)sin\gamma \cdot \gamma' \ + \ (Q_2 - Q_1)cos\gamma \qquad (11)$$

$$\cong \ l(T_1 + T_2)\gamma \ + \ (Q_2 - Q_1) \qquad \cong 0 \qquad (11')$$

Setting $M_z = 0$ in Eqn. (11') then gives the lateral tilt angle allowing pitching without yawing:

$$\gamma \ = \ \frac{(Q_1 - Q_2)}{l(T_1 + T_2)} \qquad \text{(radians)} \qquad (12)$$

The differential thrust allowing pitching without yawing is found in a similar manner, though the resulting relation is more complex. As well, Q_i in Eqns. (10) to (12) contain inertial, momentum-wheel terms $I_R\omega_i'$ in addition to the aerodynamic ones. It is therefore simpler not to include the blue decoupling/augmentation elements in the control algorithm upfront, but to allow the aircraft's attitude sensors to direct primary control (in black in Eqns. (10) and (11)) about the other axis as needed. For the result to be the same, this requires sufficiently fast attitude sensors and actuators.

3.5 Pitch Stability

Whereas roll stability and control derive from the single control element of opposed or differential longitudinal tilting – producing both gyroscopic moments and drag torques – pitch stability and pitch control are a function of the dual elements of differential thrusts and differential lateral tilting. Though not proven here, pitch stability is nevertheless possible within a large window of the parameter values. For example, while a propeller with a large MMoI about its spin axis will resist motor speed changes – and therefore inhibit dynamic pitch control from differential-thrust commands – it will enable high-speed, large-magnitude gyroscopic pitch control from differential lateral tilting.

3.6 Collective Longitudinal Tilting for Special Pitch Operations and Transition

Similar to the previous analysis of roll (Sect. 3.3), another element of control in pitch is thrust vectoring via the propellers' collective longitudinal tilting (angles β_i in Fig. 12). In this case the tilt angles will generally be different for the two propellers, but if they are the same the resulting supplemental pitch-control moment is simply

$$M_{Ty} = 2hT\sin\beta - 2I_P\beta'' \qquad (9)$$

Collective longitudinal tilting and differential thrusts can be combined in several ways to provide

- increased pitch control coupled with longitudinal motion, as in a helicopter.
- lateral motion without pitching, especially transitioning to and flying in airplane mode, (one or both propellers tilted forward 90°).
- stationary pitching, i.e., propeller disks remain in horizontal plane.

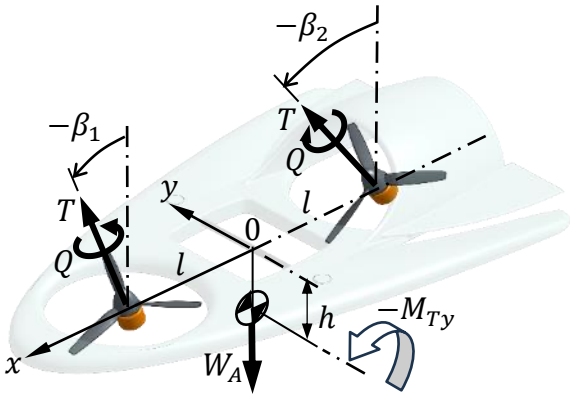

Fig. 12. Collective longitudinal tilting.

3.7 Hover Control-System Schematic

The Flyer's hover-control system comprises an onboard flight controller (Arduino APM 1280 in prior aircraft prototypes) which contains motion sensors, programmable code, and input from a command device. Figure 13 shows a typical command device of ground transmitter with human interface, and onboard receiver. Feedback to the operator of the Flyer's position etc. is not shown.

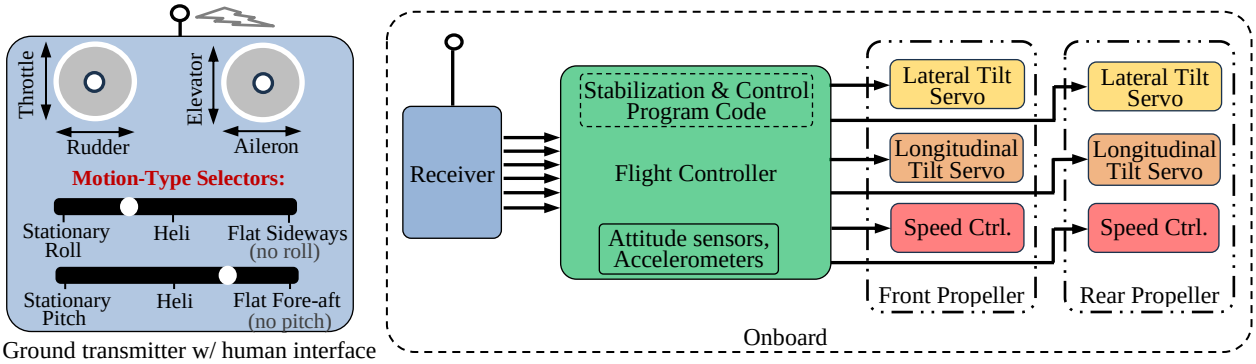

Fig. 13. Flyer's basic hover-control system with ground transmitter and human interface.

The programmable code, with its sensor/actuator gains, ensures hover stability while implementing the operator's commands through appropriate signals to the servos and speed controls. Unique to the birotor Flyer is an operator interface equipped with sliders to select the motion type, from stationary rolling and pitching to horizontal motion while remaining perfectly level.

3.8 Maturity Level of Opposed-Tilting Hover-Control Technology

Opposed active tilting has been used for more than 20 years by the author and a few others to provide birotor models with stability and control in hover. Prior to 2024, the propeller arrangement for all was lateral, or side-by-side, and so the opposed tilting was also lateral – and used primarily for aircraft pitch control. It was found early on by the author, however, that this tilting could be successfully combined with longitudinal tilting to add a thrust-vectoring element to the pitch control moments from propeller torques and gyroscopics – providing a control quality similar to a helicopter's (with its similar low center of mass). This combined or *oblique* active tilting (OAT)

can be about a single, oblique axis – e.g., the forward-bent (usually by 45 deg.) spar ends of the nVader and Nymbus models of Fig. 14 – with such tilting abbreviated as sOAT.

Fig. 14. Several of the oblique active tilting (OAT) bicopters designed and built by author.

In contrast, the larger eVader models shown in Fig. 14 employed dual-axis propeller tilting to enable 6-axis independent control. Their best hovers, however, were had by connecting the servo pairs to emulate sOAT – due to the very low mass centers of these aircraft, with thrust vectoring necessarily supplementing drag torques for good static pitch-stability. Without a programmable controller available at the time (the models carried R/C hobby heli-gyros and external mixers), 6-axis independent control was not pursued further; only the later sOAT Nymbus was equipped with a programmable controller, an Arduino APM 1280 with an inertial measurement unit (IMU). A noteworthy aside is that the Nymbus' mass center was set extremely high, almost at the plane of the propeller tilt axes (concentric with the end portions of the bent-spar, one of which is circled in Fig. 14), and so very little thrust-vector moment was involved in this stable aircraft's pitch control.

3.8.1 References for Opposed Tilting

1. Nymbus video (Calgary, 2013): https://www.youtube.com/watch?v=usiaKOpi4kE&t=1s
2. eVader on Discovery Channel (Toronto, 2007): https://vimeo.com/13925729
3. Gress, G. R., "Lift Fans as Gyroscopes for Controlling Compact VTOL Air Vehicles: Overview and Development Status of Oblique Active Tilting", AHS (now VFS) 63rd Annual Forum, May 1-3, 2007, Virginia Beach, VA.
4. Blouin, C., and Lanteigne, E., "Pitch Control of an Oblique Active Tilting Bi-rotor," International Conference on Unmanned Aircraft Systems, May 27-30, 2014, Orlando, FL.
5. Segui-Gasco, P. et al, "A Novel Actuation Concept for a Multi Rotor UAV," *Journal of Intelligent Robotic Systems*, Springer, November, 2013.
6. U.S. Patent 6,719,244 "VTOL Aircraft Control Using Opposed Tilting of Its Dual Propellers or Fans", Gary Robert Gress, 2004 (expired).

3.8.2 Application to Tandem-Configured Aircraft

The Flyer proposed in this report will be the first tandem-configured aircraft developed by the author. Some of its advantages are immediately apparent, such as the inherent pitch control available from differential thrusts, and the newly-available space for wings that do not interfere with propeller downwash – with both enabling transitions to airplane mode. There is no doubt that new issues will arise from combining a lifting body and wings with active- and transition-tilting tandem propellers, but it is strongly believed that the benefits will far outweigh the costs of resolving them.

4. Structures

The primary structure of the Flyer is the chassis sandwich-plate (Fig. 15), a rigid assembly comprised of two carbon plates separated and fastened together using metal standoffs and screws. It envelops the occupant opening, and to it are attached or integrated all the lifting and load devices:

- identical front and rear laterally-tilting tilt-arms – made largely of sandwich-plates too in the shown embodiment – the arms being longitudinally oriented to minimize drag, and their fore-aft tilting prop-motor assemblies (or propeller pods);
- landing struts (4), peripheral battery holders (4), and;
- wing spars and front shroud-structure (shown in lower-right insets of Fig. 15)

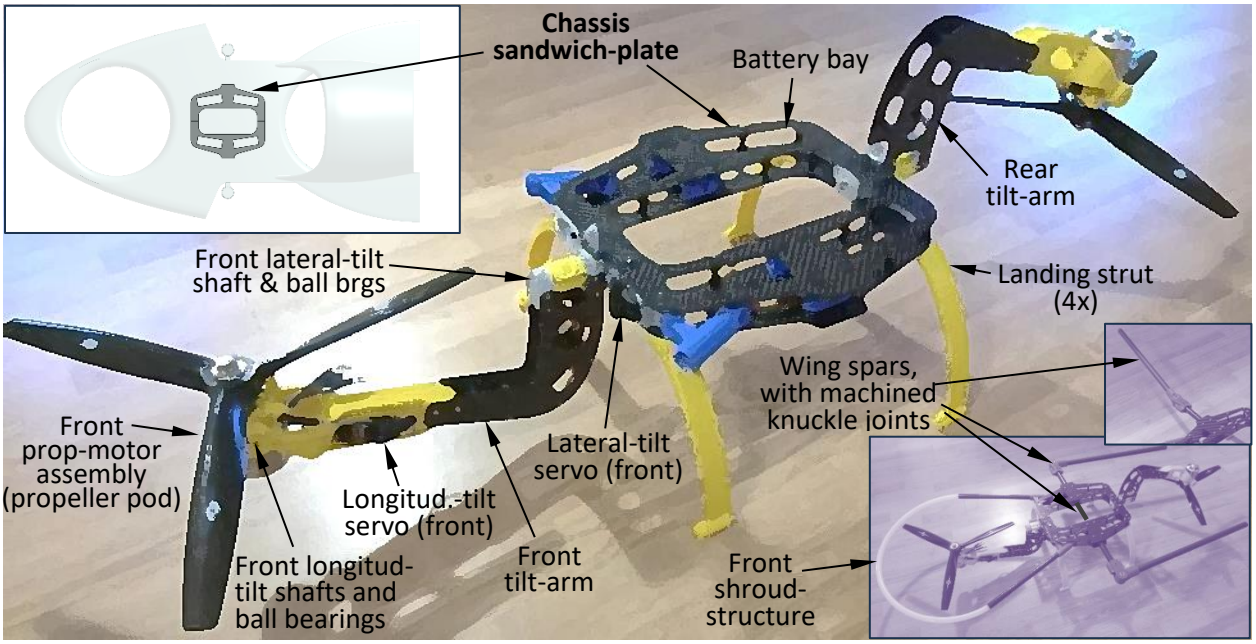

Fig. 15. Illustration of primary structure. Chassis sandwich plate (CSW) carries lift- and load-transmission devices. Insets show wing spars installed. Lower plate of CSW to be extended into payload areas (Fig. 1(d).

The remaining lifting body, half-duct and wing surfaces – and underlying support structures –are considered secondary, intended to handle mostly-local air pressure differentials. Suitable construction materials and methods are considered to include:

- plywood skin and ribs
- thermoformed plastic skin and foam core
- Laid-up or vacuum-bagged fiberglass skin and foam core.

5. Performance

5.1 Hover Endurance

The following endurance estimation assumes a motionless hover out of ground effect (OGE).

5.1.1 Propellers: Modifications and the Fan-in-Wing Effect

Using dimensional analysis, eVader data from Ref. 3 can be directly extrapolated to estimate the hover power required and endurance of the GoAERO Flyer. However, since the full-scale propellers will not belong to the same family as the eVader's, an opportunity arises to better suit them to the application. Specifically, to improve hover performance, the chord of the Flyer's propeller blades have been hypothetically increased by 50% relative to the eVader family of geometrically similar propellers. Dimensional analysis predicts the shaft power (and RPM) to be reduced from that family's by a factor of 1.5, but the relation for shaft torque to remain the same:

$$P_h = 15.2\,\frac{T^{3/2}}{R} \quad , \quad Q_h = 0.271\,R \cdot T \qquad (13)$$

where P_h is in Watts, Q_h in Nm, R in ft, and T in lb.

With its large range of parameter values and its custom engineering, *Sensenich Propeller Co.* appears to be worthwhile engaging for the design and manufacture of the Flyer's props – including the checking of fatigue failure, considering its active-tilting control means. As Fig. 16 shows, their propellers come in several blade counts, and their pitches are fixed or ground-adjustable.

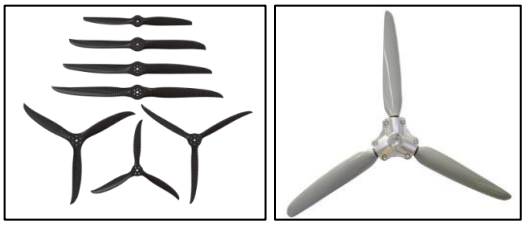

Fig. 16. *Sensenich Propeller Co.* fixed-pitch & ground-adjustable composite props. Dia. from 15 to 98 in, powers from 5 to 200HP. 2-, 3-, 4-, 5-, and 6-blade.

Equation (13) applies to standard atmosphere, and its use in the endurance calculations assumes that installation losses in the aircraft are the same as those encountered in the measurement test rig. This means that any effect of the Flyer's half-duct on rear propeller performance is assumed to be negligible (a fair assumption based on testing of the author's GoFly aircraft), and that T from Eqn. (13) could be equated to half the aircraft's total weight W_T. There is, however, at least one other factor at play, one which contributes a positive vertical lift: the *fan-in-wing* (FIW) effect of a propeller embedded in a wing or body with a rounded inlet. It is a result of ambient air being dawn across the wing's surface – at less than ambient pressure – towards the propeller opening. From classical momentum theory and Bernoulli's theorem, this lifting force on an infinite surface is simply ϵT, where $\epsilon \cong 0.13$. Using half this value (which assumes an obstruction-free zone 0.3R wide around the opening) – to allow for the Flyer's physical constraints and configuration – gives

$$(1 + 0.065)T = 0.5W_T \quad \rightarrow \quad T = 0.47W_T \qquad (14)$$

For reference, the measured FIW effect of the GoFly aircraft (0.5 lb extra lift for a W_T of 11 lb) was $0.048T$, which, in comparison to the full, ideal value 0.13T, is commensurate with the half-envelopment of the 13-in diameter propellers by the wide-chord canard. It is also worth noting that the power reduction due to the FIW effect on the 48-in propellers in the current proposed Flyer is equivalent to using larger, free propellers of diameter 52.7 in. (from Eqn. (13)).

5.1.2 Motors and Batteries

Shaft power P_h and torque Q_h from Eqn. (13) can be rewritten in terms of aircraft total weight using (14). Efficiency η_m for the motor/controller gives the electrical power consumed P_m as well:

$$P_h = 4.9\,\frac{{W_T}^{3/2}}{R} \text{ (W)} \quad , \qquad P_m = \frac{1}{\eta_m}\,P_h \quad , \qquad Q_h = 0.127\,R \cdot W_T \text{ (Nm)} \qquad (15)$$

Hover OGE endurance of the aircraft, as a function of its battery capacity $\mathcal{C}$, is simply

$$t_h = 60\,\frac{(1-\mu)\mathcal{C}}{2P_m} \text{ (minutes)} \quad , \qquad \text{where} \qquad \mathcal{C} = \varepsilon\,\frac{W_B(lb)}{2.2\ lb/kg} \text{ (W·h)} \qquad (16)$$

and where μ is the fraction of energy that must remain in the batteries upon discharge (= the minimum *state of charge* (SoC)). ε is the battery system's energy density in W·h/kg, and W_B is its weight in lb. **Writing the total aircraft weight W_T as the sum of the airframe-plus-payload weight W_{T0} and battery weight W_B**, and combining this with Eqns. (15) and (16) gives endurance in terms of the propeller, motor and battery parameters:

$$t_h = 6.2\eta_m R\,\frac{(1-\mu)\mathcal{C}}{\left(W_{T0}+2.2\frac{\mathcal{C}}{\varepsilon}\right)^{3/2}} = 7.9\,\frac{\mathcal{C}}{(W_{T0}+0.0073\mathcal{C})^{3/2}} \text{ (minutes)} \qquad (17)$$

where the right hand expression uses the following parameter values in addition to R = 2 ft: an efficiency η_m of 0.92 is typical of the eVTOL motors/controllers made by *MagiDrive* (Fig. 17); at least two manufacturers of lithium-ion batteries for eVTOL aircraft, *Amprius* and *Magnix*, offer energy densities ε of 300 W·h/kg, with *Amprius* recommending a minimum SoC, μ, of 0.3. Both battery brands have a maximum discharge rate of $10\mathcal{C}$, so that $2P_m \leq 10\mathcal{C}$, which from Eqn. (15) gives the capacity constraint

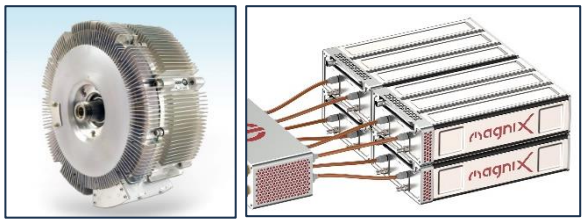

Fig. 17. *Left*: Magidrive prop motor by *Magicall Inc.*, whose tables are used to select appropriate size in later section. *Right*: 300S eVTOL Lithium-ion battery modules by *Magnix*.

$$\mathcal{C}_{min} = 0.98\frac{{W_T}^{3/2}}{\eta_m R} = 0.53{W_T}^{3/2} \quad (18)$$

5.1.3 GoAERO Missions and Stationary-Hover Endurance Plot

Knowing that the longest of the maximum allowed flight times in GoAERO Missions 2 and 3 is 30 min., and that the payload for each mission is the 125 lb. 'Alex' mannequin, gives a single battery-charge condition that endurance Eqn. (17) can be plotted around. These missions occur not far from the operations zone, so the above hover calculations apply for their entirety. Mission 1 is more complex, and likely involves swapping in fresh batteries and possibly extending the variable-sweep wings – and so is dealt with more fully in a later section. In that mission, however, taking off and landing quickly with larger payloads – up to 320 lb. – can be desirable, which provides another condition to consider. To guide selection of a range of parameter values for the endurance plot, shown in Fig. 18, use was made of the rule of thumb that the airframe, payload and battery weights are roughly equal, i.e., each weighs roughly $W_T/3$. Also included in the endurance plot are lines of constant propeller speed N_h, which is readily obtained from Eqns. (13) or (15):

$$N_h = \frac{60}{2\pi}\frac{P_h}{Q_h} = 540\frac{T^{1/2}}{R^2} = 370\frac{W_T^{1/2}}{R^2} \quad \text{(RPM)} \quad (19)$$

5.1.4 Aircraft Weight Estimate and Hover Design Points

Based on the author's prior work with hovering aircraft, which are usually overdesigned and overweight, it is estimated that a 35% scale model of the Tandem-X Flyer – without batteries or payload – will weigh less 12 lb. Using geometric scaling, this translates to an full-size airframe weight equal to about 275 lb., represented by the dashed, vertical line in Fig. 18. This will be taken to be the working estimate for subsequent performance calculations here, but an allowance of another 75 lb. (for an empty weight of 350 lb., equivalent to a 35%-scale model weight of 15 lb.), will be kept in mind, and any substantial difficulties noted. In some cases, empty-weight increases beyond 275 lb. will require operation with a different class of motors and other items, and these are considered to be absorbed in the extra 75 lb. allowance. There is no doubt that accuracy regarding the actual weight will improve as development continues.

Point 1 in Fig. 18 is considered the aircraft's primary design point, representing continuous operation in GoAERO Missions 2 and 3, with: 125 lb. payload (W_{T0} = 275+125 = 400 lb.); motors running at P_h = 50 kW but rated at 60 kW max continuous (e.g., MagiDrive Model 75) for a 20% take-off margin; and total battery weight of W_B= 350 lb (so W_T = 750 lb.); giving a hover endurance of t_h = 18.3 minutes, which is acceptable considering that the missions involve spending considerable time on the ground or carrying no payload. A design-loci curve is passed through point 1, showing how the Flyer's weight might change if it were designed precisely for some other point. Nevertheless, the as-designed Flyer with its 'Alex' payload can operate anywhere along the vertical W_{T0} = 400 lb. line, just non-optimally and subject to limitations.

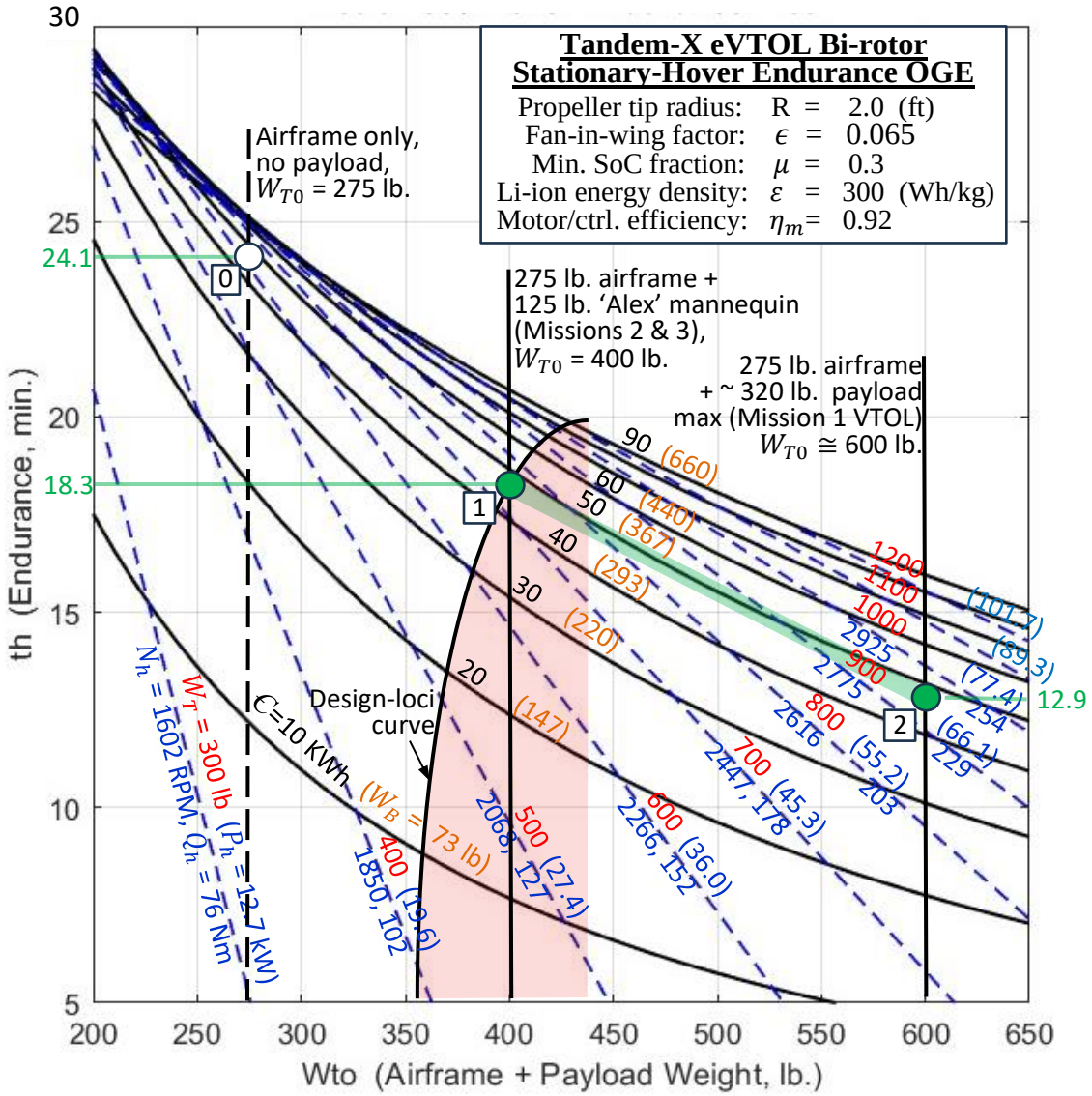

Fig. 18. Stationary-hover endurance graph for Tandem-X Flyer, with GoAero-mission operating points 0, 1 and 2 using same 350-lb Li-ion battery. From Eqns. (15)-(19). P_h is the power of just one of the two motors.

In order for the Flyer to perform successfully in the overall GoAERO challenge, consideration must also be given to the its Mission 1, or Productivity Mission. Considering that the forward speeds of the Flyer in hover mode are unknown, and that there will be little margin for error, hover-mode operation in this mission should be limited to just its VTOL portions, so designing for it can be secondary or non-optimum. There is, however, advantage to carrying the largest permissible payload of 320 lb. and so minimizing the number of flight segments and associated time involved (minimum number of loaded segments = 1250 lb/320 lb per segment ≅ 4) . This then locates a secondary-operation vertical line at W_{T0} = 600 lb. (= 275 + 320, rounded). Using the same battery (W_B = 350 lb.) as for operating point 1 then gives a total weight of W_T = 950 lb for the take off and landing part of Mission 1 (point 2 in Fig. 18), with a total endurance of 12.9 minutes and a corresponding required power of each motor at P_h = 70 kW. This puts the MagiDrive Model 75 prop-motors in the 30-second "short duration" realm, but which appears sufficient to complete each loaded take off and landing operation of Mission 1. Eight take-offs and landings (4 segments x 2) at 30 sec. each totals 4 min., which leaves 12.9 – 4 = 8.9 minutes of point-2 energy remaining

for the horizontal-flight portions of the mission and also its zero-payload segments. Using the same 350-lb battery for the zero-payload segments of Mission 1 corresponds to operating point 0 in Fig. 18 (W_T = 625 lb.), for which the total endurance is 24.1 minutes. Eight take-off and landings in this condition takes 4 minutes as well, but corresponds to only $4\times(625/950)^{1.5}$ = 2.1 minutes of point-2 energy being consumed, leaving 8.9 – 2.1 = 6.8 min. at that state.

5.2 Lifting-Body Performance

The following sub-sections will determine the energy required for the remaining, horizontal-flight portions of Mission 1. The degree and efficiency to which the Flyer's semi-elliptical body planform contributes lift and offloads the propellers in forward flight has been estimated and plotted by applying low-aspect-ratio adjustments – derived from extant analysis of aircraft dorsal fins – to conventional wing theory. Simplified by ignoring the propeller openings, half-duct and other details, the analysis and its results are shown in Fig. 19.

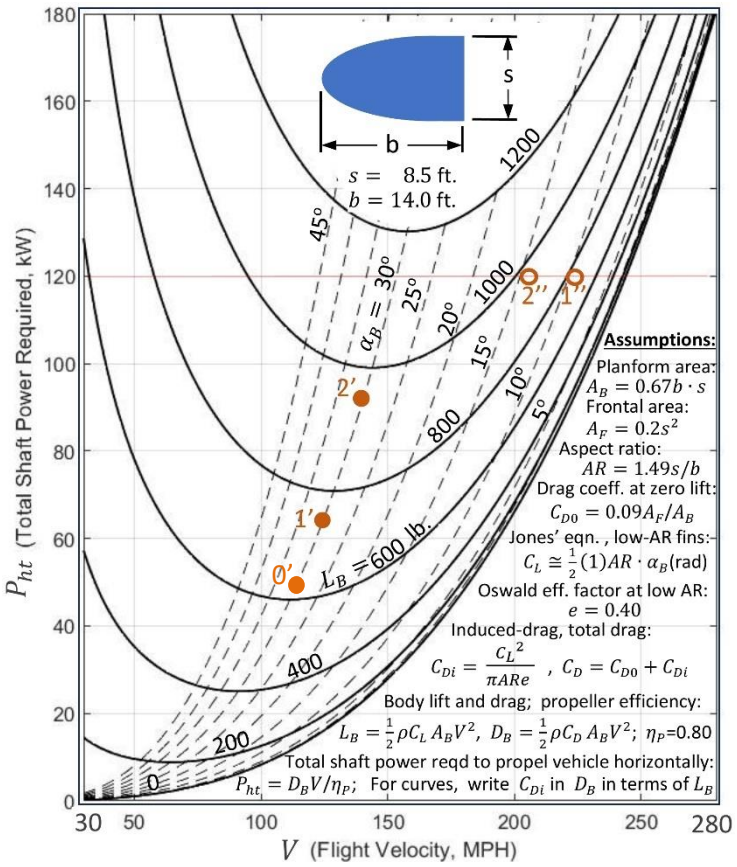

Fig. 19. Total shaft power P_{ht} required to propel lifting body vs. horizontal flight velocity V for various lifts L_B and corresponding angles of attack α_B.

5.2.1 Improved Endurance in Flight

The plot shows the 750-lb design-point-1 aircraft can be fully lifted by the body – with the least-power/max-endurance being at point 1′, corresponding to an angle of attack $\alpha_B = 30^o$. Though likely not useful for Missions 2 or 3, the associated forward speed is 113 mph, with a total shaft power (to hypothetical, horizontal-axis props) of 63 kW – considerably less than the 100 kW needed to hover (pt. 1 in Fig. 18). Figure 19's point 2′ shows a similar power offloading for the 950-lb Mission 1 application. But perhaps more importantly, Fig. 19 shows that the body does provide some lift assistance at low V and α_B in hover mode for less total power.

5.2.2 High-Speed Dash

Another feature of the lifting body is the high-speed dash capability that it enables. At the maximum-continuous total shaft power of 120 kW for the MagiDrive Model 75 motors, both the 750-lb and 950-lb aircraft can attain speeds of over 200 mph (points 1″ and 2″, respectively, in Fig. 19) – assuming of course that the propeller speeds and/or pitches can be suitably increased to provide the necessary propulsive thrusts. If so, for the same power, the Flyer in lifting-body mode is calculated to be faster than the extended-wing version in this regime and beyond.

5.2.3 Endurance and Range Still Not Sufficient

Nevertheless, though the points in Fig. 19 show the Flyer's endurance and range to be improved by operating it as a lifting body, those improvements are not sufficient to eliminate substantial battery swapping when participating in Mission 1 of the GoAERO challenge. This is the reason for the Flyer's extendable wings, whose performance is investigated in the following section.

5.3 Extended-Wing Performance

The performance of the Flyer with its wings extended was estimated by treating them as a conventional wing (dark blue shape in Fig. 20 inset) of the same span s_w. The Flyer's body was assumed to be horizontal and providing no lift – regardless of the wing angle of attack α_w – but its zero-lift drag (from the previous section) has been added to the wing's. The analysis and its results are shown and plotted in Fig. 20.

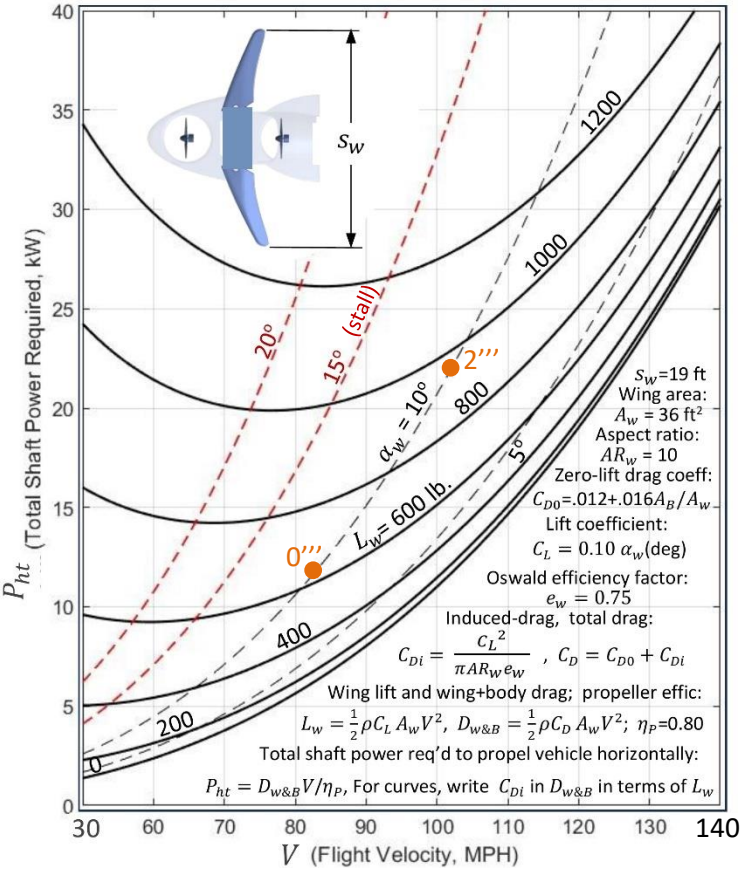

Fig. 20. Total shaft power P_{ht} required to propel extended-wing Flyer vs. horizontal flight velocity V for various lifts L_w and corresponding wing angles of attack α_w. Body is horizontal throughout.

5.3.1 Extended Range

With the Flyer operating at a stall-safe α_w of 10°, the plot shows a substantial reduction in the total power required; the 950-lb Mission 1 configuration (pt. 2‴, V=102 mph) needs only 22 kW – compared to 140 kW for hover (pt. 2 in Fig. 18). And the zero-payload configuration (pt. 0‴ , V=82 mph) requires only 11.6 kW. Dividing each of the two powers by its respective flight speed, summing the results, and dividing the energy remaining after the Mission 1 takeoffs and landings (6.8 minutes x 140 kW, from the end of Sect. 5.1.4) by this sum, gives a travel distance of 44.4 miles each way (loaded one way, empty the other). This is considerably more than the 6 miles needed each way for a Mission 1 load of 1250 lb. (1250/320 ≅ 4 segments, x 1.5 miles per segment each way) So, it appears that the Flyer can perform far more take offs and landings – and run far more segments – on a single battery charge than originally thought. A quick calculation shows that the single battery will last a good part of the Mission 1 90-minute time limit.

5.4 Tandem-X's Propellers: Manipulation Within, and Between, Flight Modes

In all modes of the Flyer's operation – hover, lifting-body, and extended-wing – the propellers' tilts and speeds can be manipulated to assist those operations and to enable or make smoother the transitions between them. As such, especially in the case of automatic, programmed manipulation, the stall regime so common in airplanes can be made non-existent in the Tandem-X. And the disconnect between modes at low flight speeds – evident upon inspection of the prior performance plots – can be eliminated with similar manipulation. Future control and performance analysis should include simultaneous propeller manipulation with wing or lifting-body operation. For example, in extended-wing mode, considering the low power usually required, the front propeller need not be tilted forward at all (despite the Fig. 20 inset showing both propellers tilted forward 90 degrees), but it could be used to adjust pitch trim in the aircraft. And both propellers in lifting-body mode can be just partly tilted, thereby assisting with vertical lift as well as providing forward thrust.

6. Specifications and Drawings

Flyer Specifications for GoAero Prize, Missions 1,2 & 3

Empty wt:	275 lb (125 kg)	
Li-Ion batt.	350 lb (160 kg) @ 300 Wh/kg	(Magnix)
Disc area:	25.1 ft^2 (2.33 m^2) total	
Motors:	(2) 60 kW rated ea	(Magidrive 75, wt ~15 kg ea)
Propellers	(2) 4-ft 3bl, CW/CCW, >1.6 kg ea	(Sensenich custom)
Tilt servos:	(4) 220 Nm & 65 deg/sec ea	(Lynxmotion LSS-P-M1, 4.5 kg)
Endurance:	18.3 min. hover w 125 lb 'Alex' -	Missions 2 & 3
	12.9 min. hover w 320 lb -	Maximum Mission 1 payload
or	82.1 min. airplane @ 102 mph =	140 mi. range w same payload
	(actual Mission 1 will combine both VTOL and airplane flight)